Please cite this article in press as: Umetsu et al., Local Increases in Mechanical Tension Shape Compartment Boundaries by Biasing Cell Intercalations, Current Biology (2014), http://dx.doi.org/10.1016/j.cub.2014.06.052

Current Biology *24*, 1–8, August 4, 2014 ©2014 Elsevier Ltd All rights reserved http://dx.doi.org/10.1016/j.cub.2014.06.052

Report

Local Increases in Mechanical Tension Shape Compartment Boundaries by Biasing Cell Intercalations

Daiki Umetsu,[1,4] Benoît Aigouy,[2,5] Maryam Aliee,[3,6] Liyuan Sui,[1] Suzanne Eaton,[2] Frank Jülicher,[3] and Christian Dahmann[1,*]

[1]Institute of Genetics, Technische Universität Dresden, 01062 Dresden, Germany

[2]Max Planck Institute of Molecular Cell Biology and Genetics, Pfotenhauerstrasse 108, 01307 Dresden, Germany

[3]Max Planck Institute for the Physics of Complex Systems, Nöthnitzer Strasse 38, 01187 Dresden, Germany

Summary

Mechanical forces play important roles during tissue organization in developing animals. Many tissues are organized into adjacent, nonmixing groups of cells termed compartments [1–7]. Boundaries between compartments display a straight morphology and are associated with signaling centers that are important for tissue growth and patterning [8]. Local increases in mechanical tension at cell junctions along compartment boundaries have recently been shown to prevent cell mixing and to maintain straight boundaries [9–13]. The cellular mechanisms by which local increases in mechanical tension prevent cell mixing at compartment boundaries, however, remain poorly understood. Here, we have used live imaging and quantitative image analysis to determine cellular dynamics at and near the anteroposterior compartment boundaries of the *Drosophila* pupal abdominal epidermis. We show that cell mixing within compartments involves multiple cell intercalations. Frequency and orientation of cell intercalations are unchanged along the compartment boundaries; rather, an asymmetry in the shrinkage of junctions during intercalation is biased, resulting in cell rearrangements that suppress cell mixing. Simulations of tissue growth show that local increases in mechanical tension can account for this bias in junctional shrinkage. We conclude that local increases in mechanical tension maintain cell populations separate by influencing junctional rearrangements during cell intercalation.

Results and Discussion

We analyzed cellular dynamics of compartmentalization in the pupal abdominal epidermis of *Drosophila*, a useful system for live imaging [14]. The dorsal part of this epithelial tissue is subdivided into a sequence of anterior and posterior compartments [15]. Each compartment is derived from an initially separate histoblast nest that proliferates and fuses with neighboring nests to form the anteroposterior compartment boundaries (AP boundaries) and to build a continuous epithelial sheet (Figure 1A and Movie S1 available online) [14].

Time Evolution of the Shape of the AP Boundary in *Drosophila* Histoblast Nests

We first revealed the dynamics of the shape of the AP boundary. We labeled adherens junctions in histoblast nests using a fusion protein of DE-Cadherin and GFP [16], performed time-lapse imaging, and used image analysis software [17] to identify cell junctions (Figure 1A and Movie S1). Cell junctions along the AP boundary were identified by tracing of cell lineages of anterior and posterior histoblast nests. As control, we arbitrarily defined seven adjacent regions at increasing distances to the AP boundary, separated by lines parallel to the AP boundary (Figure 1B), and traced cell lineages in these regions during development (see the Supplemental Experimental Procedures). We characterized the shape of these lines (henceforth referred to as "control interfaces") and the AP boundary by a geometric measure termed "roughness" [9, 10]. The roughness of the control interfaces in histoblast nests increased over a 3 hr period (Figures 1B–1E, Movie S2). By contrast, the roughness of the AP boundary remained nearly constant over time (Figures 1B–1E). Thus, consistent with previous simulations of tissue growth [9], the roughness of control interfaces increases with time, whereas the roughness of the AP boundary is maintained nearly constant during development.

Dynamics of Cells along the AP Boundary Is Constrained

Mosaic analysis has established that cells between adjacent compartments do not mix; i.e., a cell from one compartment will never become completely surrounded by cells from the adjacent compartment [18]. The absence of cell mixing between compartments may be a mere consequence of the inability of cells within compartments to change their neighbors during development. To test this notion, we analyzed the dynamics of cells along control interfaces and compared it to the dynamics of cells along the AP boundary. To quantify cell mixing behavior, we determined the fraction of the adherens junctional length of histoblast cells that are in contact with cells of the adjacent region or compartment (termed "cell mixing index," γ; Figure 2A) over time. For $\gamma = 0$, a cell is only in contact with cells of the same region or compartment, whereas for $\gamma = 1$, a cell is only in contact with cells of the neighboring region or compartment. The average values of the cell mixing indices for cells along control interfaces and the AP boundary were similar (Figures S1A and S1B). However, whereas the maximal value of the observed cell mixing index for cells along the AP boundary was 0.58, cells located along control interfaces had a cell mixing index of up to 1.0 (Figures S1A and S1B). Consistently, we observed cells along control interfaces whose cell mixing index was initially low but increased up to 1.0 within 1–2 hr (Figure 2B). These results confirm that histoblast cells from adjacent compartments do not mix and establish that histoblast cells within a compartment exchange their neighbors during development, resulting in cell mixing. The cell mixing index is a geometric measure that also reflects the local shape of the AP boundary. We will

[4]Present address: RIKEN Center for Developmental Biology, Kobe 650-0047, Japan

[5]Present address: Institut de Biologie du Développement de Marseille, 13288 Marseille Cedex 9, France

[6]Present address: Laboratoire Reproduction et Développement des Plantes and Laboratoire Joliot-Curie, Université de Lyon, 69365 Lyon Cedex 7, France

*Correspondence: christian.dahmann@tu-dresden.de

Please cite this article in press as: Umetsu et al., Local Increases in Mechanical Tension Shape Compartment Boundaries by Biasing Cell Intercalations, Current Biology (2014), http://dx.doi.org/10.1016/j.cub.2014.06.052

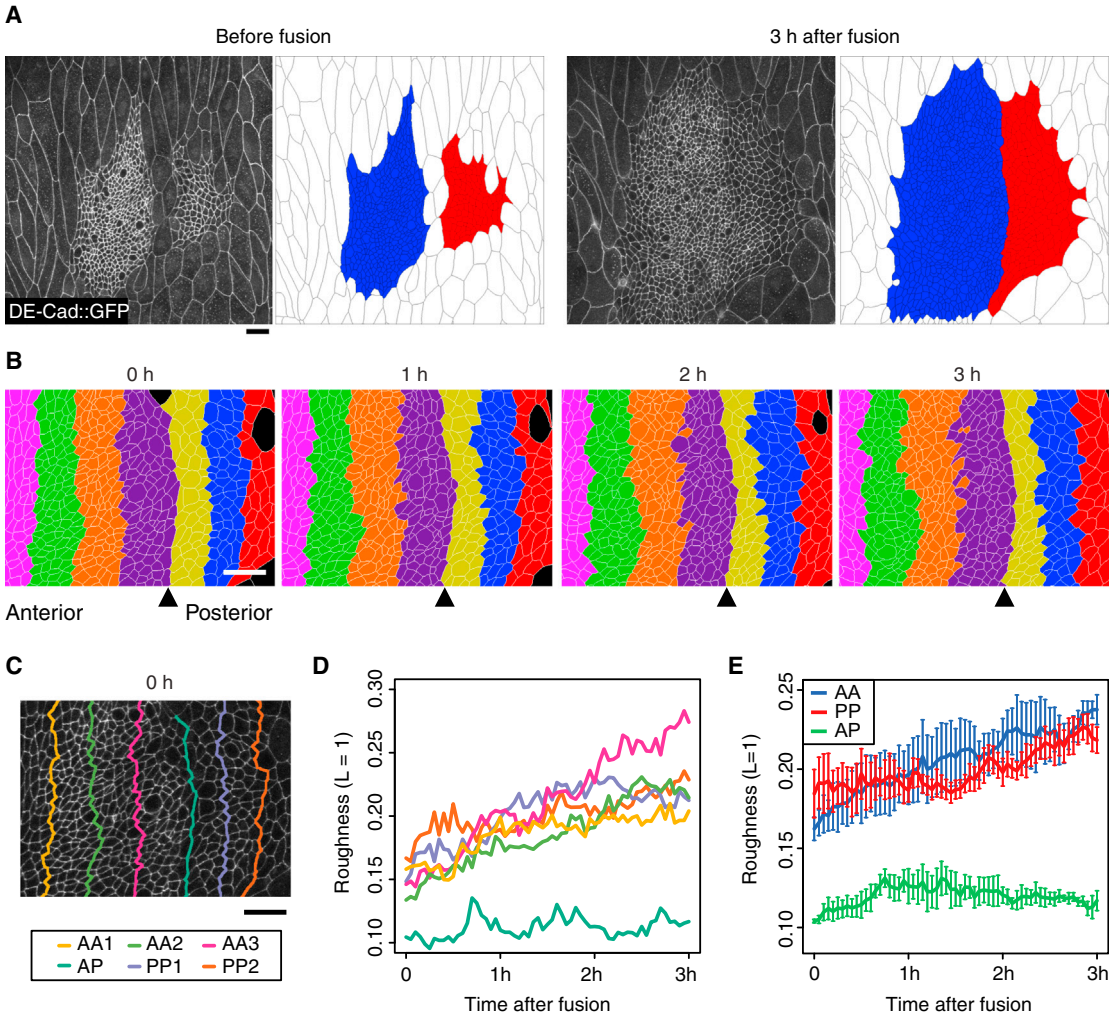

Figure 1. Time Evolution of the Shape of the AP Boundary in *Drosophila* Histoblast Nests

(A) Images of anterior and posterior dorsal histoblast nests before fusion (left) and 3 hr after fusion (right). Cell junctions are visualized by DE-Cad::GFP. Segmented images of anterior (blue) and posterior (red) dorsal histoblast nests are shown to the right of each image. Anterior is to the left and posterior is to the right unless otherwise stated in this and all the following figures.

(B) Lineage tracing of seven regions parallel to the AP boundary. Time after the fusion of histoblast nests is shown on top of each image. Anterior compartment is divided into four regions (from left to right: magenta, green, orange, and purple) and posterior compartment is divided into three regions (yellow, blue, and red).

(C) Snapshot of the shapes of the interfaces between neighboring regions at the time of histoblast nest fusion. Interfaces between neighboring groups in (B) are referred to as AA1, AA2, AA3, AP, PP1, and PP2 from anterior to posterior.

(D) Time evolution of roughness of the interfaces between neighboring regions for the distance, L, of one average cell junction length. The roughness is defined as the average distance of excursions of the interface away from a straight line for different lengths of the line [9, 10]. Interfaces between neighboring groups are as in (C).

(E) Time evolution of roughness of control interfaces between neighboring regions within the anterior (AA) and posterior (PP) compartments and of the AP boundary for the distance, L, of one average cell junction length. Error bars indicate the SEM. n = 12 (AA), n = 8 (PP), and n = 4 (AP) interfaces of four animals. Scale bars represent 20 μm.

therefore use the cell mixing index as a measure for both local AP boundary shape and cell mixing.

To test how cell mixing across the AP boundary is prevented and how the straight shape of the AP boundary is maintained, we analyzed changes in cell mixing index at 3 min intervals. At control interfaces, the cell mixing index increased or decreased with equal probabilities (Figure 2C). Cells at the AP boundary that had a small cell mixing index ($0.3 \leq \gamma < 0.4$) also increased or decreased their cell mixing index with equal probabilities (Figure 2C). Interestingly, for cells along the AP boundary displaying high cell mixing indices ($0.4 \leq \gamma < 0.6$), the probability to decrease cell mixing index was much greater than the probability to increase cell mixing index (Figure 2C). Similarly, the cell mixing index of cells along the border of en^E mutant clones of cells located in the posterior compartment (Figure S1C) preferentially decreased when initial cell mixing index was large (Figure 2C). en^E is a deletion of the *engrailed* and *invected* selector genes, which are specifically expressed in posterior cells and whose activities are required to prevent cell mixing across the AP boundary [15, 19]. Moreover, cell mixing index of cells along the AP boundary fluctuated less over longer time intervals (1 hr) and stayed below an upper limit (Figures S1D–S1G). We conclude that in response to the selector genes *engrailed* and *invected*, the

Please cite this article in press as: Umetsu et al., Local Increases in Mechanical Tension Shape Compartment Boundaries by Biasing Cell Intercalations, Current Biology (2014), http://dx.doi.org/10.1016/j.cub.2014.06.052

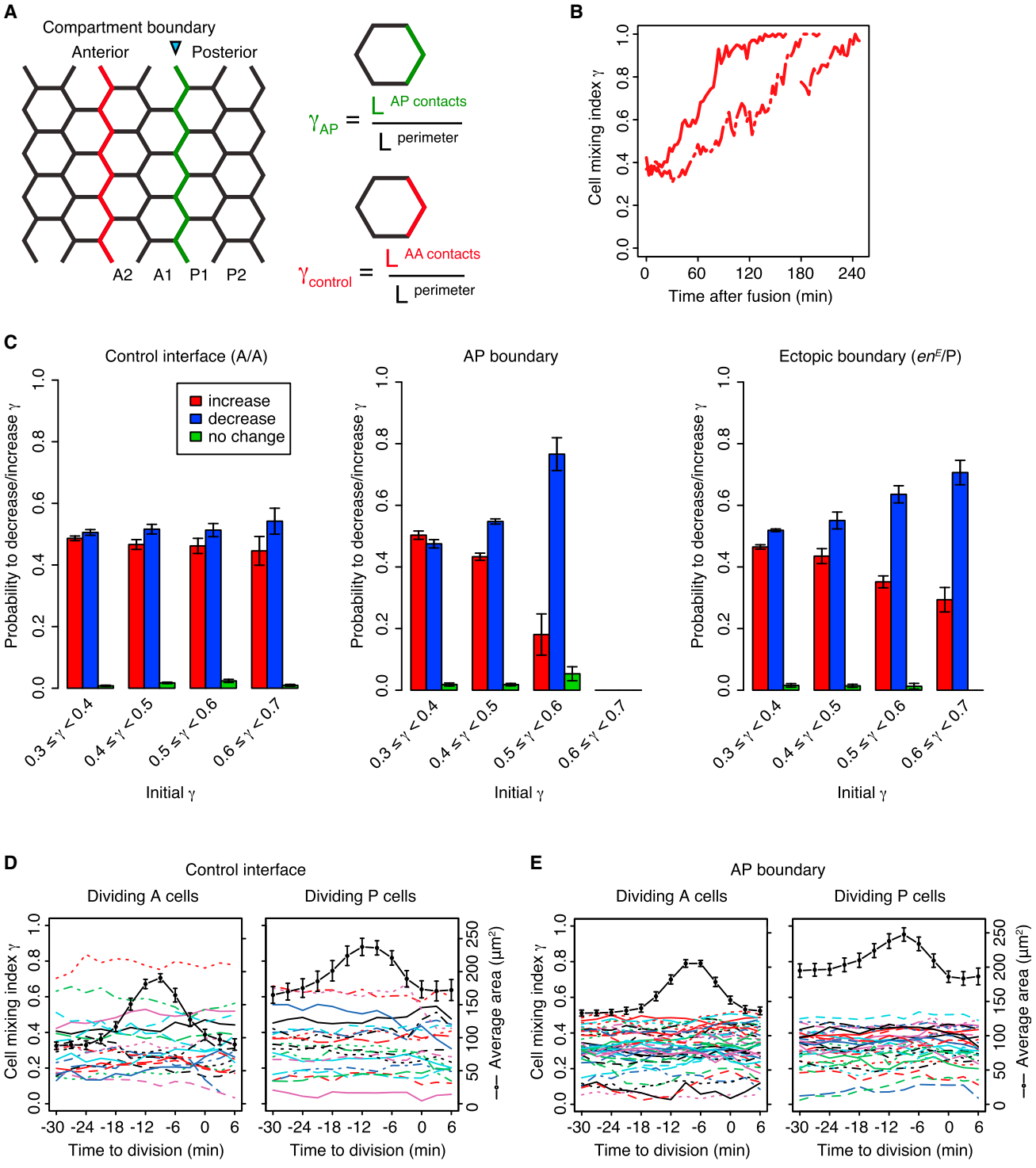

Figure 2. Dynamics of Cells along the AP Boundary Is Constrained

(A) Definition of the cell mixing index, γ. The cell mixing index is the fraction of the perimeter of a cell that is shared with cells from a neighboring compartment or region (AP contacts and AA contacts). The cell mixing index was determined for the first row of anterior (A1) and posterior (P1) cells that are located along the AP boundary (green) and control anterior cells that are located along control interfaces shown in Figure 1C (red).

(B) Time evolution of the cell mixing index for three single cells located at control interfaces.

(C) Probability to increase (red), to decrease (blue), or not to change (green) the cell mixing index, γ, in a 3 min time window. Data were collected for individual cells in consecutive time windows for each movie. Cells with $0.3 \leq \gamma < 0.4$, $0.4 \leq \gamma < 0.5$, $0.5 \leq \gamma < 0.6$, and $0.6 \leq \gamma < 0.7$ were separately analyzed. A/A indicates junctions between two anterior cells (n = 3,271, 2,784, 1,683, and 764 cells for $0.3 \leq \gamma < 0.4$, $0.4 \leq \gamma < 0.5$, $0.5 \leq \gamma < 0.6$, and $0.6 \leq \gamma < 0.7$, respectively). AP indicates junctions between anterior and posterior cells (n = 2,420, 2,125, 151, and 0 cells for $0.3 \leq \gamma < 0.4$, $0.4 \leq \gamma < 0.5$, $0.5 \leq \gamma < 0.6$, and $0.6 \leq \gamma < 0.7$, respectively). en^E/P indicates the junction between en^E mutant posterior cells and wild-type posterior cells (n = 2,595, 1,174, 240, and 20 cells for

(legend continued on next page)

dynamics of cells along the AP boundary is constrained. Cells tend to reduce their contact to cells from the neighboring compartment until it falls below an upper limit. As a consequence, mixing of anterior and posterior cells is suppressed. The minimization of contact for large, but not for small, cell mixing indices provides a mechanism that allows two compartments to have a common interface, yet limits the contact of cells from the two compartments to maintain a straight boundary.

T1 Transitions of Cells Can Promote Cell Mixing within Compartments

To further understand the cellular mechanisms that prevent cell mixing between two compartments, we first sought to identify the processes that result in cell mixing within compartments. Studies in the *Drosophila* embryonic epidermis have emphasized the role of cell divisions in promoting cell mixing and have indicated that the AP boundary is challenged by "pushing" of dividing cells into the adjacent compartment [13]. To quantitatively test this notion in histoblast nests, we measured the cell mixing index of dividing cells. Notably, cells dividing at control interfaces or the AP boundary did not significantly change their cell mixing index (Figures 2D and 2E). Thus, in histoblast nests cell division does not directly promote cell mixing and cells dividing at the AP boundary do not "push" into the neighboring compartment.

Cell mixing at control interfaces was accompanied by multiple cell intercalations that involved the sequential loss and gain of junctions (Figure 3A). During these intercalations, termed T1 transitions [20], the shrinkage of a junction shared by two cells into a four-way vertex is followed by the formation of a new junction resulting in a new pair of neighbor cells (Figure 3B). T1 transitions lead to cell neighbor exchange and thus could contribute to cell mixing within compartments. To test this notion, we measured the change in cell mixing index of cells undergoing T1 transitions. We distinguished between T1 transitions in which cells gained a new junction along the AP boundary or control interface (ON boundary, Figure 3B) and those in which cells gained a new junction perpendicular to it (OFF boundary). Cells along control interfaces on average increased their cell mixing index when they gained an ON boundary junction (Figures 3C and 3D). Interestingly, cells along the AP boundary undergoing T1 transitions did on average not increase their cell mixing index, regardless of whether they gained an ON boundary or OFF boundary junction (Figures 3C, 3D, and S2A). These data demonstrate that T1 transitions contribute to cell mixing within compartments. Importantly, they also show that cell mixing is suppressed for T1 transitions along the AP boundary.

T1 Transitions of Cells along the AP Boundary Are Biased to Suppress Cell Mixing

To reveal the mechanism that suppresses cell mixing for T1 transitions along the AP boundary, we quantitatively analyzed the frequency, orientation, and geometry of T1 transitions. We only considered T1 transitions gaining ON boundary junctions, because mainly those T1 transitions contributed to cell mixing (Figure 3D and Figure S2A). The frequency and orientation of T1 transitions was indistinguishable for cells along the AP boundary and for cells of the anterior compartment (Figures S2B–S2D and Movie S3). We noticed, however, that the junction shrinkage associated with T1 transitions was frequently asymmetric throughout the tissue. One of the two vertices at the ends of the shrinking junction moved predominantly (Movie S4). For T1 transitions of cells along the AP boundary, the predominant movement of the vertex located *away* from the AP boundary would result in the new junction emerging from the four-way vertex in a way that the straight shape of the AP boundary is little or not disturbed (Figure 3E, case 1). Predominant movement of the vertex located *along* the AP boundary, on the other hand, would result in the local distortion of the AP boundary (Figure 3E, case 2). To quantify the result of junctional shrinkage, we measured the position of the new cell junction emerging from the four-way vertex (Figure 3E). For T1 transitions of cells along control interfaces, the new cell junction was on average centered between the pair of cells that lost their junctions (Figures 3C and 3F and Movie S4). By contrast, for cells along the AP boundary, junctions along the AP boundary were less deformed, resulting in the positioning of the new junction closer to the side of the AP boundary (Figures 3C and 3F and Movie S4). Similarly, for cells along en^E mutant clone borders, junctions along the clone border were less deformed during T1 transitions, resulting in the positioning of the new junction closer to the side of the clone border (Figures 3C and 3F). Finally, junctions along the AP boundary in larval wing discs, which are also under increased mechanical tension [10], were also less deformed during T1 transitions (Figure 3F, Figure S2E, Movie S5). Similar observations were made when, instead of the position of the new cell junction, the angles of the junctions connected to the four-way vertex were measured (Figure S2F). These data demonstrate that the movement of the vertex located along the AP boundaries is restrained during the junctional shrinkage of T1 transitions in both histoblasts and wing discs. This bias in the asymmetry of junctional shrinkage results in a cell configuration that suppresses cell mixing and maintains the straight shape of the AP boundaries.

Local Increases in Mechanical Tension Bias T1 Transitions of Cells along the AP Boundary

We next analyzed the mechanisms by which the asymmetry of junctional shrinkage is biased during T1 transitions. Local increases in mechanical tension have been demonstrated along the AP and dorsoventral boundaries in *Drosophila* wing discs [9, 10]. Such local increases in mechanical tension could result in the shortening of cell junctions and thus could bias the shrinkage of cell junctions. We therefore first tested whether mechanical tension at cell junctions is increased along the AP boundary of histoblast nests. To determine mechanical tension, we ablated single cell junctions and quantified the initial velocity of the displacement of vertices at the ends of ablated cell junctions, which is a relative measure of mechanical tension (Figures 4A and S3A) [21]. The initial velocity in response to ablation of cell junctions in the anterior or

$0.3 \leq \gamma < 0.4$, $0.4 \leq \gamma < 0.5$, $0.5 \leq \gamma < 0.6$, and $0.6 \leq \gamma < 0.7$, respectively). Error bars indicate the SEM. Four (A/A), four (A/P), and six (en^E/P) animals were analyzed.

(D and E) Plots of cell mixing indices for individual dividing cells and the average area of dividing cells as a function of time to cell division for anterior and posterior cells located at the control interface (D) and AP boundary (E). Error bars indicate the SEM. n = 56 anterior and n = 38 posterior cells at the control interfaces of four animals, and n = 20 anterior and n = 20 posterior cells at the AP boundary of one animal.

See also Figure S1.

Please cite this article in press as: Umetsu et al., Local Increases in Mechanical Tension Shape Compartment Boundaries by Biasing Cell Intercalations, Current Biology (2014), http://dx.doi.org/10.1016/j.cub.2014.06.052

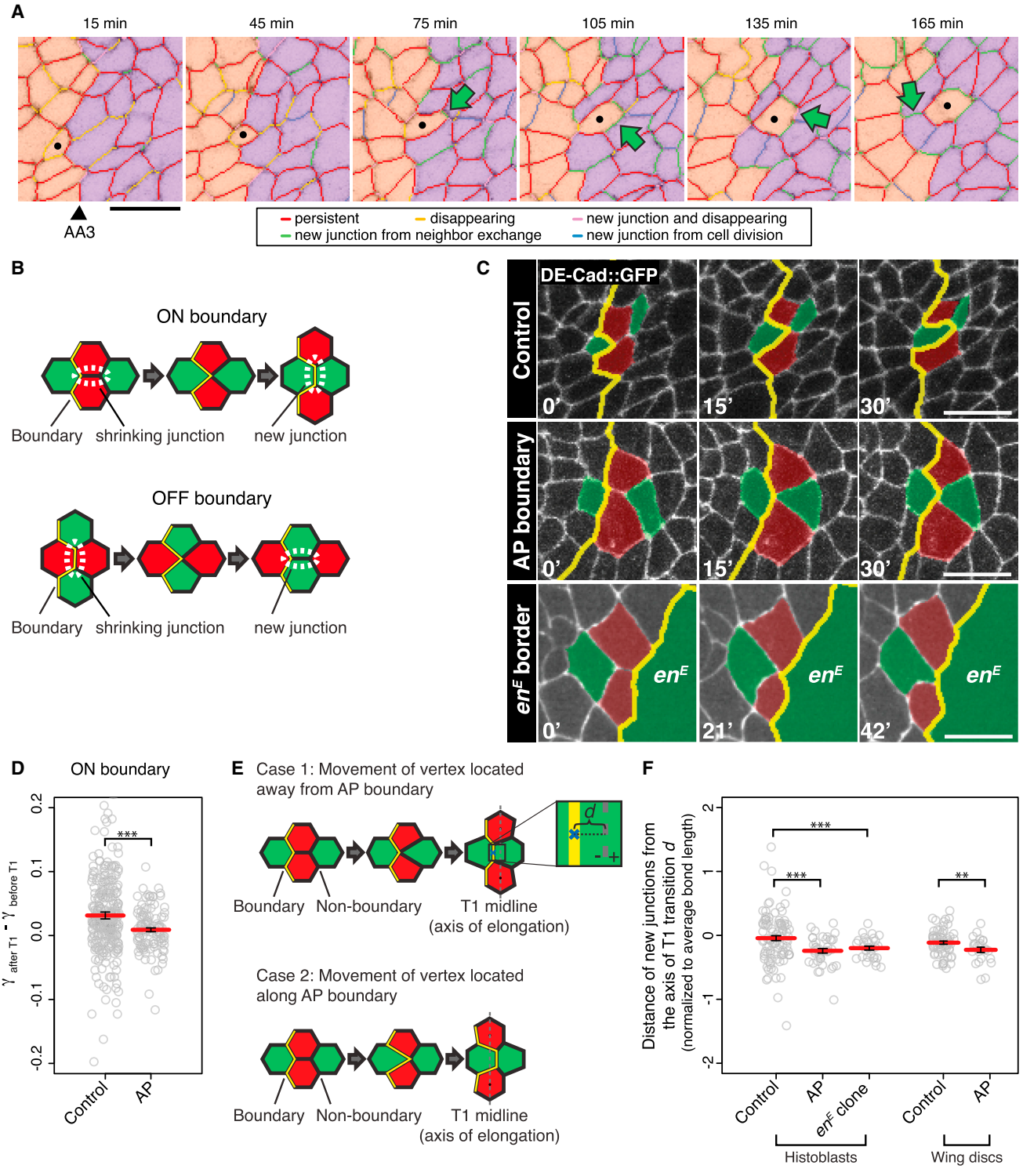

Figure 3. T1 Transitions along the AP Boundary Are Biased to Disfavor Cell Mixing

(A) Snapshots of a cell (marked with a black dot) that is going to mix with a neighboring group of cells (purple) at control interface AA3, as shown in Figures 1B and 1C. Cell junctions generated by T1 transitions are indicated by arrows. The color of junction codes for the appearance and disappearance of junctions throughout the time course as shown at the bottom. The scale bar represents 10 μm.

(B) Schematic representation of sequential topological changes during T1 transitions. The T1 transition involves four cells. Two cells that are initially in contact (depicted in red) lose the cell junction between them, and the remaining two cells (green) come in contact to generate a new junction. The T1 transition can be oriented in such a way that the new junction forms along the compartment boundary (ON boundary, top) or at an angle to the compartment boundary (OFF boundary, bottom).

(C) Time series of T1 transitions at a control interface, the AP boundary, and borders of en^E mutant clones located in the posterior compartment. Cells are color coded as indicated in (B). Scale bars represent 10 μm or 5 μm (en^E border).

(legend continued on next page)

posterior compartments was comparable (Figure 4B). By contrast, the initial velocity of vertex displacement upon ablation of AP cell junctions or cell junctions along borders of en^E clones was increased approximately 2-fold (Figure 4B). Thus, mechanical tension at cell junctions is locally increased approximately 2-fold along the AP boundary and at en^E clone borders in histoblast nests.

To test whether local increases in mechanical tension are sufficient to bias junctional shrinkage during T1 transitions, we performed simulations of the growth of a tissue with two compartments using a vertex model [9, 10, 22]. In this vertex model, stable configurations of a network of junctions depend on physical parameters, including mechanical tension at cell junctions. We ran simulations using relative mechanical tension at cell junctions along the boundary between compartments as compared to the bulk of the tissue of $\lambda = 1$, 2, and 3 (Figure 4C). We then, similarly to the experiment, analyzed the geometry of T1 transitions for cells along the boundary. In the reference scenario, the new junction was placed on average on the axis of the T1 transition (Figure 4D). By contrast, for $\lambda = 2$ and $\lambda = 3$, the new junction was placed more closely to the compartment boundary (Figure 4D). For $\lambda = 2$, the new junctions were placed in the simulation at a comparable distance to the axis of T1 transition as in the experiment (compare Figures 3F and 4D). Similar observations were made when, instead of the position of the new cell junction, the angles of the junctions connected to the four-way vertex were measured (Figure S3B). A bias in junctional shrinkage was observed for a range of values of the physical parameters used in the simulations (Figures S3C–S3H). Consistent with these simulations, we furthermore show, based on theoretical considerations of force balances, that unequal tension acting on cell junctions results in an asymmetric shrinkage that leads to a four-way vertex positioned toward the junction with higher tension (see the Supplemental Experimental Procedures). We conclude that the local 2-fold increase in mechanical tension can account for the bias in the asymmetry of junctional shrinkage during T1 transitions along the AP boundary.

Conclusions

We have used live imaging and quantitative image analysis to demonstrate for the first time differences in the dynamics of cells and junctions along a compartment boundary in a highly proliferative tissue. We show that cell mixing within a compartment is promoted by multiple junctional rearrangements involving T1 transitions (Figure 4E). We propose that along the AP boundary in histoblast nests, the differential expression of the *engrailed* and *invected* selector genes in the posterior and anterior compartments results in a local increase of mechanical tension at cell junctions (Figure 4F). This local increase in mechanical tension influences neither the frequency nor the orientation of T1 transitions. Rather, the local increase in mechanical tension biases the asymmetry of junctional shrinkage during T1 transitions. Increased mechanical tension resists deformations of junctions along the AP boundary. As a consequence, junctions at an angle to the AP boundary shrink during T1 transitions by the predominant movement of the vertex located away from the compartment boundary. This results in a cell configuration that suppresses cell mixing and maintains the straight shape of the AP boundary. It will be interesting to identify the molecular basis for this cellular behavior. Signatures of local increases in mechanical tension have been observed at several compartment boundaries and other interfaces separating cells within tissues [9, 10, 13, 23–26]. We therefore propose that the bias of junctional rearrangements by local increases in mechanical tension might be a general mechanism to separate groups of cells in developing animals.

Supplemental Information

Supplemental Information includes Supplemental Experimental Procedures, three figures, and five movies and can be found with this article online at http://dx.doi.org/10.1016/j.cub.2014.06.052.

Acknowledgments

This work was initiated while D.U. and C.D. were at the Max Planck Institute of Molecular Cell Biology and Genetics (MPI-CBG). We thank the MPI-CBG imaging facility for providing access to imaging equipment and S. Grill and M. Nishikawa for providing their laser ablation system. We thank K. Rudolf, F. Aurich, C. Gogdas, F.P. Herrmann, S. Jedlicka, R. Kindermann, S. Lübke, and A.-C. Stuhr for help with image processing, Y. Hong for fly stocks, and G. Salbreux and S. Grill for comments on the manuscript. This work was supported by the Japan Society for the Promotion of Science (D.U.) and the Deutsche Forschungsgemeinschaft (DA586/10, DA586/13-1, and DA586/14 to C.D.).

Received: January 12, 2014
Revised: May 28, 2014
Accepted: June 19, 2014
Published: July 24, 2014

References

1. Batlle, E., and Wilkinson, D.G. (2012). Molecular mechanisms of cell segregation and boundary formation in development and tumorigenesis. Cold Spring Harb. Perspect. Biol. *4*, a008227.
2. Dahmann, C., Oates, A.C., and Brand, M. (2011). Boundary formation and maintenance in tissue development. Nat. Rev. Genet. *12*, 43–55.
3. Monier, B., Pélissier-Monier, A., and Sanson, B. (2011). Establishment and maintenance of compartmental boundaries: role of contractile actomyosin barriers. Cell. Mol. Life Sci. *68*, 1897–1910.
4. Tepass, U., Godt, D., and Winklbauer, R. (2002). Cell sorting in animal development: signalling and adhesive mechanisms in the formation of tissue boundaries. Curr. Opin. Genet. Dev. *12*, 572–582.
5. Kiecker, C., and Lumsden, A. (2005). Compartments and their boundaries in vertebrate brain development. Nat. Rev. Neurosci. *6*, 553–564.
6. Martin, A.C., and Wieschaus, E.F. (2010). Tensions divide. Nat. Cell Biol. *12*, 5–7.
7. Vincent, J.P., and Irons, D. (2009). Developmental biology: tension at the border. Curr. Biol. *19*, R1028–R1030.

(D) Difference in cell mixing index for cells located at control interfaces or the AP boundary before and after T1 transitions that give rise to new junctions along the boundary (ON boundary). Only cells that were already located at the control interface or the AP boundary before the T1 transition were analyzed. Error bars indicate the SEM. n = 296 (control) and n = 120 (AP) cells of four animals. ***$p < 0.01$.

(E) Schematic representation of two cases of asymmetric intercalation. The midline of T1 transition is defined by connecting centroids of a pair of cells that lose contact (red).

(F) Asymmetry of intercalations of pupal histoblast and larval wing disc cells. Positions of new junctions formed by T1 transitions were analyzed with respect to the midline of T1 transition (see E). The distance, *d*, between the new junction and the midline is negative when the new junction is located to the side where the AP boundary is present and is positive when the new junction is located to the opposite side (see schematic in inset of E). Error bars indicate the SEM. n = 103 (control) and n = 40 (AP) T1 transitions in one pupa, n = 30 (en^E clone) T1 transitions in four pupae, and n = 48 (control) and n = 24 (AP) T1 transitions in five wing discs. ***$p < 0.01$, **$p < 0.03$.

See also Figure S2.

Please cite this article in press as: Umetsu et al., Local Increases in Mechanical Tension Shape Compartment Boundaries by Biasing Cell Intercalations, Current Biology (2014), http://dx.doi.org/10.1016/j.cub.2014.06.052

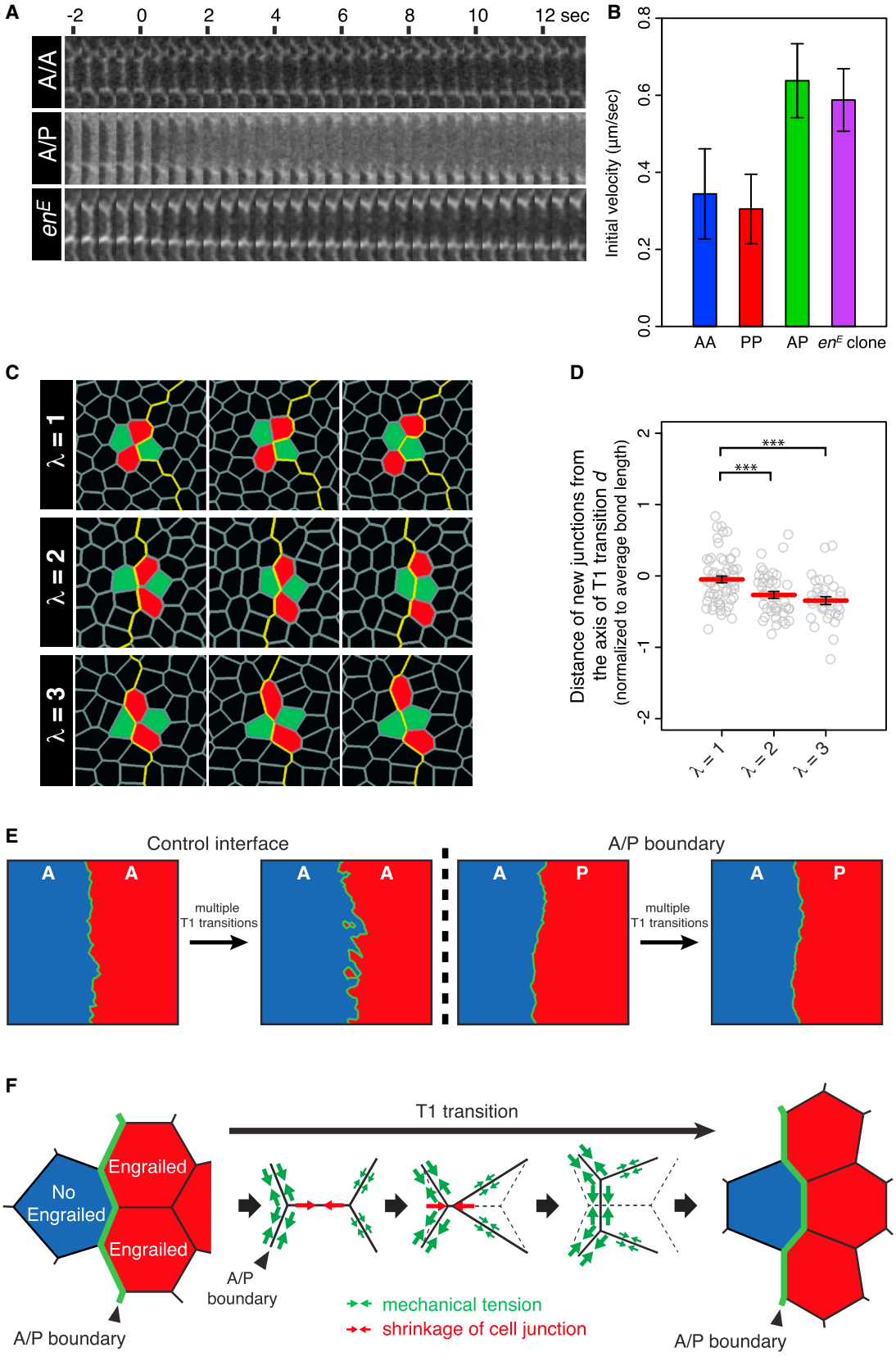

Figure 4. Local Increases in Mechanical Tension Bias T1 Transitions along the AP Boundary

(A) Kymograms of cell junctions between anterior cells (A/A), at the AP boundary (A/P), and at borders of *en*^{E} clones visualized by DE-Cad::GFP before and after laser ablation.

(legend continued on next page)

8. Dahmann, C., and Basler, K. (1999). Compartment boundaries: at the edge of development. Trends Genet. *15*, 320–326.
9. Aliee, M., Röper, J.C., Landsberg, K.P., Pentzold, C., Widmann, T.J., Jülicher, F., and Dahmann, C. (2012). Physical mechanisms shaping the *Drosophila* dorsoventral compartment boundary. Curr. Biol. *22*, 967–976.
10. Landsberg, K.P., Farhadifar, R., Ranft, J., Umetsu, D., Widmann, T.J., Bittig, T., Said, A., Jülicher, F., and Dahmann, C. (2009). Increased cell bond tension governs cell sorting at the *Drosophila* anteroposterior compartment boundary. Curr. Biol. *19*, 1950–1955.
11. Major, R.J., and Irvine, K.D. (2005). Influence of Notch on dorsoventral compartmentalization and actin organization in the *Drosophila* wing. Development *132*, 3823–3833.
12. Major, R.J., and Irvine, K.D. (2006). Localization and requirement for Myosin II at the dorsal-ventral compartment boundary of the *Drosophila* wing. Dev. Dyn. *235*, 3051–3058.
13. Monier, B., Pélissier-Monier, A., Brand, A.H., and Sanson, B. (2010). An actomyosin-based barrier inhibits cell mixing at compartmental boundaries in *Drosophila* embryos. Nat. Cell Biol. *12*, 60–65, 1–9.
14. Ninov, N., Chiarelli, D.A., and Martín-Blanco, E. (2007). Extrinsic and intrinsic mechanisms directing epithelial cell sheet replacement during *Drosophila* metamorphosis. Development *134*, 367–379.
15. Kornberg, T. (1981). Compartments in the abdomen of *Drosophila* and the role of the *engrailed* locus. Dev. Biol. *86*, 363–372.
16. Huang, J., Zhou, W., Dong, W., Watson, A.M., and Hong, Y. (2009). From the Cover: Directed, efficient, and versatile modifications of the *Drosophila* genome by genomic engineering. Proc. Natl. Acad. Sci. USA *106*, 8284–8289.
17. Aigouy, B., Farhadifar, R., Staple, D.B., Sagner, A., Röper, J.C., Jülicher, F., and Eaton, S. (2010). Cell flow reorients the axis of planar polarity in the wing epithelium of *Drosophila*. Cell *142*, 773–786.
18. Garcia-Bellido, A., Ripoll, P., and Morata, G. (1973). Developmental compartmentalisation of the wing disk of *Drosophila*. Nat. New Biol. *245*, 251–253.
19. Lawrence, P.A., Casal, J., and Struhl, G. (1999). The hedgehog morphogen and gradients of cell affinity in the abdomen of *Drosophila*. Development *126*, 2441–2449.
20. Stavans, J. (1993). The evolution of cellular structures. Rep. Prog. Phys. *56*, 733–789.
21. Mayer, M., Depken, M., Bois, J.S., Jülicher, F., and Grill, S.W. (2010). Anisotropies in cortical tension reveal the physical basis of polarizing cortical flows. Nature *467*, 617–621.
22. Farhadifar, R., Röper, J.C., Aigouy, B., Eaton, S., and Jülicher, F. (2007). The influence of cell mechanics, cell-cell interactions, and proliferation on epithelial packing. Curr. Biol. *17*, 2095–2104.
23. Röper, K. (2012). Anisotropy of Crumbs and aPKC drives myosin cable assembly during tube formation. Dev. Cell *23*, 939–953.
24. Gettings, M., Serman, F., Rousset, R., Bagnerini, P., Almeida, L., and Noselli, S. (2010). JNK signalling controls remodelling of the segment boundary through cell reprogramming during *Drosophila* morphogenesis. PLoS Biol. *8*, e1000390.
25. Simone, R.P., and DiNardo, S. (2010). Actomyosin contractility and Discs large contribute to junctional conversion in guiding cell alignment within the *Drosophila* embryonic epithelium. Development *137*, 1385–1394.
26. Osterfield, M., Du, X., Schüpbach, T., Wieschaus, E., and Shvartsman, S.Y. (2013). Three-dimensional epithelial morphogenesis in the developing *Drosophila* egg. Dev. Cell *24*, 400–410.

(B) Initial velocity of vertex displacement after laser ablation of cell junctions of the indicated types. en^E clone refers to cell junctions along borders of en^E mutant clones located in the posterior compartment. Error bars indicate the SEM. n = 13 (AP), n = 13 (AA), n = 13 (PP), and n = 23 (en^E clone) cell junctions.
(C) Examples of configurations of networks in simulations of tissue growth with two compartments for different values of λ. Pictures from left to right show the sequence of configurations during a T1 transition. The yellow line marks compartment boundary. Color coding of cells is as in Figure 3B.
(D) Asymmetry of intercalations in simulations. Positions of new junctions formed by T1 transitions were analyzed with respect to the midline of T1 transition (see Figure 3E). Error bars indicate the SEM. n = 59 ($\lambda = 1$), n = 45 ($\lambda = 2$), and n = 34 ($\lambda = 3$) T1 transitions. ***$p < 0.01$.
(E) Scheme illustrating the influence of multiple T1 transitions on the shape of a control interface and the AP boundary (green lines).
(F) Model depicting the cellular mechanisms shaping the AP boundary in histoblast nests. Apposition of posterior cells expressing the selector genes *engrailed* and *invected* and anterior cells that do not express these selector genes results in the local increase in mechanical tension at cell junctions along the AP boundary. Increased mechanical tension at the junctions along the AP boundary results in their reduced deformation during T1 transitions. As a consequence, the asymmetry of junctional shrinkage during T1 transitions is biased in such a way that the junction shrinks predominantly by the movement of the vertex located away from the AP boundary. The new junction emerges from the four-way vertex at a location where the straight shape of the AP boundary is little or not disturbed.
See also Figure S3.